

TDM-R1: Reinforcing Few-Step Diffusion Models with Non-Differentiable Reward

Yihong Luo¹, Tianyang Hu², Weijian Luo³ and Jing Tang^{4,1}

¹Hong Kong University of Science and Technology, ²The Chinese University of Hong Kong, Shenzhen, ³hi-Lab, Xiaohongshu Inc,

⁴Hong Kong University of Science and Technology (Guangzhou)

While few-step generative models have enabled powerful image and video generation at significantly lower cost, generic reinforcement learning (RL) paradigms for few-step models remain an unsolved problem. Existing RL approaches for few-step diffusion models strongly rely on back-propagating through differentiable reward models, thereby excluding the majority of important real-world reward signals, e.g., non-differentiable rewards such as humans' binary likeness, object counts, etc. To properly incorporate non-differentiable rewards to improve few-step generative models, we introduce TDM-R1, a novel reinforcement learning paradigm built upon a leading few-step model, Trajectory Distribution Matching (TDM). TDM-R1 decouples the learning process into surrogate reward learning and generator learning. Furthermore, we developed practical methods to obtain per-step reward signals along the deterministic generation trajectory of TDM, resulting in a unified RL post-training method that significantly improves few-step models' ability with generic rewards. We conduct extensive experiments ranging from text-rendering, visual quality, and preference alignment. All results demonstrate that TDM-R1 is a powerful reinforcement learning paradigm for few-step text-to-image models, achieving state-of-the-art reinforcement learning performances on both in-domain and out-of-domain metrics. Furthermore, TDM-R1 also scales effectively to the recent strong Z-Image model, consistently outperforming both its 100-NFE and few-step variants with only 4 NFEs. Project page: <https://github.com/Luo-Yihong/TDM-R1>.

1. Introduction

Achieving rapid, high-fidelity image and video generation continues to be a fundamental objective in the field of Artificial Intelligence Generated Content (AIGC). Recent advancements in few-step generative models, e.g., diffusion distillation (Luo et al., 2023, 2024a, 2025c; Xie et al., 2024b; Yin et al., 2023; Zhou et al., 2024), have shown successes in ultra-fast photo-realistic images and videos generation with accelerations up to 50 times that of diffusion models. With ultra-fast generation efficiency and leading performances, few-step models are becoming a standard with large-scale serving in industry products (Cai et al., 2025; Labs, 2024). *Despite significant gains in speed and visual fidelity, few-step models still struggle with certain challenges, e.g., precise instruction following, complicated text rendering, and proper object positioning.*

In recent years, reinforcement learning has shown significant ability in improving deep learning models' specialized abilities, ranging from large language models (Bai et al., 2022; DeepSeek-AI, 2025; Ouyang et al., 2022; Shao et al., 2024; Ziegler et al., 2019), standard diffusion models (Liu et al., 2025; Xue et al., 2025b), to few-step generative models (Luo, 2024; Luo et al., 2025a,b; Ren et al., 2024). It is expected that proper RL paradigms are capable of addressing the mentioned challenges of few-step image or video generation.

Though existing papers have explored RL methods for few-step generative models (Luo, 2024; Luo et al., 2025a; Ren et al., 2024), their algorithms rely on a narrow assumption:

- *they require reward signals to be differentiable, such that the outputs of the few-step generative models are able to backpropagate through the rewards.*



Figure 1 | Samples generated by **TDM-R1** using only 4 NFEs, obtained by reinforcing the recent powerful Z-Image model (Team et al., 2025).

Such a narrow requirement clearly excludes a vast array of essentially non-differentiable reward signals, such as human binary preferences in real-world cases, discrete object counts, and correctness of text-rendering via OCR models. On the other side, as pointed out by representative processes in LLM, e.g., Deepseek-R1 (DeepSeek-AI, 2025), rapid successes of RL in large language models clearly indicate the importance of generic non-differential rewards in unlocking models' hidden potentials.

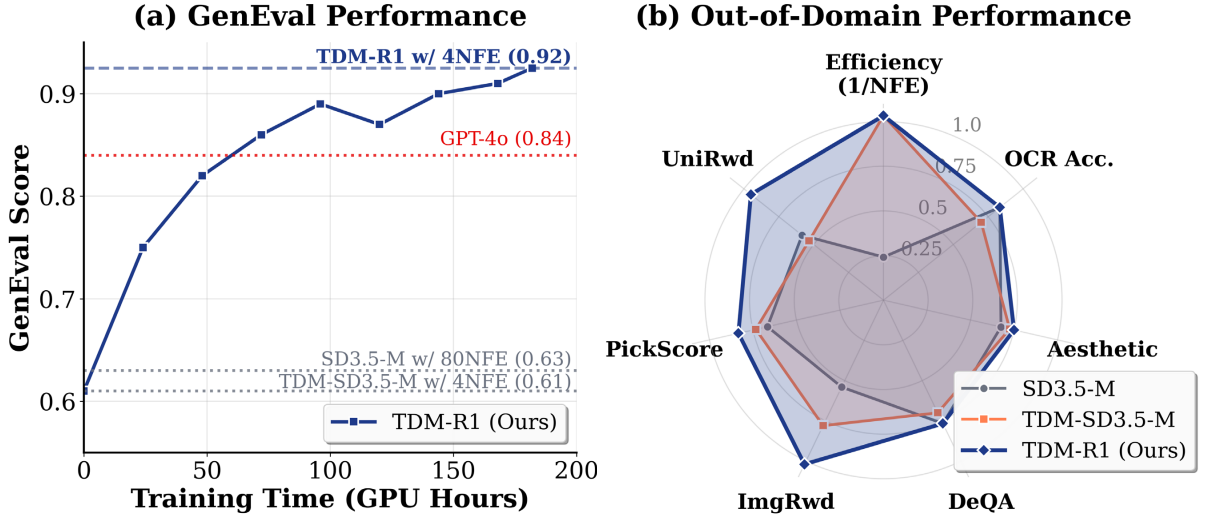


Figure 2 | **TDM-R1** rapidly boosts GenEval score of few-step TDM, notably outperforming its many-step base model and GPT-4o. This is achieved without sacrificing out-of-domain metrics.

To solve the key problem of *using non-differentiable rewards*, we introduce **TDM-R1**, a novel reinforcement learning paradigm designed to reinforce these few-step models using *free-form non-differentiable reward feedback* without requiring additional ground-truth image data. **TDM-R1** is built upon Trajectory Distribution Matching (TDM) (Luo et al., 2025c), a typical few-step generative model. The core idea of TDM-R1 is to utilize the deterministic trajectories of TDM to assign rewards to intermediate denoising steps via an efficient and unbiased reward estimate for every sample along the trajectory. We also propose a diffusion-parameterized dynamic surrogate reward trained using pairwise groups to provide stable RL supervision at each step.

By decoupling the learning process into surrogate reward learning and generator optimization, TDM-R1 enables few-step models to achieve performance levels that even surpass many-step counterparts. In Section 4, we conduct extensive experiments across compositional image generation, ranging from visual text rendering and human preference alignment to validate the superiority of TDM-R1 on both in-domain and out-of-domain metrics. **Remarkably, our method enables models to outperform expensive 80-NFE base models using only 4 NFE.** Most notably, on the rigorous GenEval benchmark (Ghosh et al., 2023), TDM-R1 boosts performance from 61% to 92%—significantly surpassing the 80-NFE base model (63%) and the commercial state-of-the-art GPT-4o (84%). Beyond SD3.5-M, TDM-R1 also scales to the powerful 6B-parameter Z-Image model (Team et al., 2025), surpassing both its 100-NFE and few-step variants across in-domain and out-of-domain metrics with only 4 NFEs.

2. Preliminaries

Diffusion Models. Diffusion Models (DMs) (Ho et al., 2020; Sohl-Dickstein et al., 2015) establish a forward diffusion process that corrupts input sample \mathbf{x}_0 with Gaussian noise over T discrete timesteps. This forward process is defined by: $q(\mathbf{x}_t|\mathbf{x}) \triangleq \mathcal{N}(\mathbf{x}_t; \alpha_t\mathbf{x}, \sigma_t^2\mathbf{I})$, where α_t and σ_t are hyperparameters regarding the noise schedule. At any given timestep, noisy samples are generated as $\mathbf{x}_t = \alpha_t\mathbf{x} + \sigma_t\epsilon$, with $\epsilon \sim \mathcal{N}(\mathbf{0}, \mathbf{I})$. The learned reverse diffusion process is formulated as $p_\psi(\mathbf{x}_{t-1}|\mathbf{x}_t) \triangleq \mathcal{N}(\mathbf{x}_{t-1}; \mu_\psi(\mathbf{x}_t, t), \eta_t^2\mathbf{I})$. Training proceeds by optimizing the neural network f_ψ through the denoising objective

$$\mathbb{E}_{\mathbf{x}, \epsilon, t} \lambda_t \|f_\psi(\mathbf{x}_t, t) - \mathbf{x}\|_2^2. \quad (1)$$

A well-trained diffusion model can estimate the score via: $\nabla_{\mathbf{x}_t} \log p_t(\mathbf{x}_t) \approx s_\psi(\mathbf{x}_t) = -\frac{\mathbf{x}_t - \alpha_t f_\psi(\mathbf{x}_t, t)}{\sigma_t^2}$.

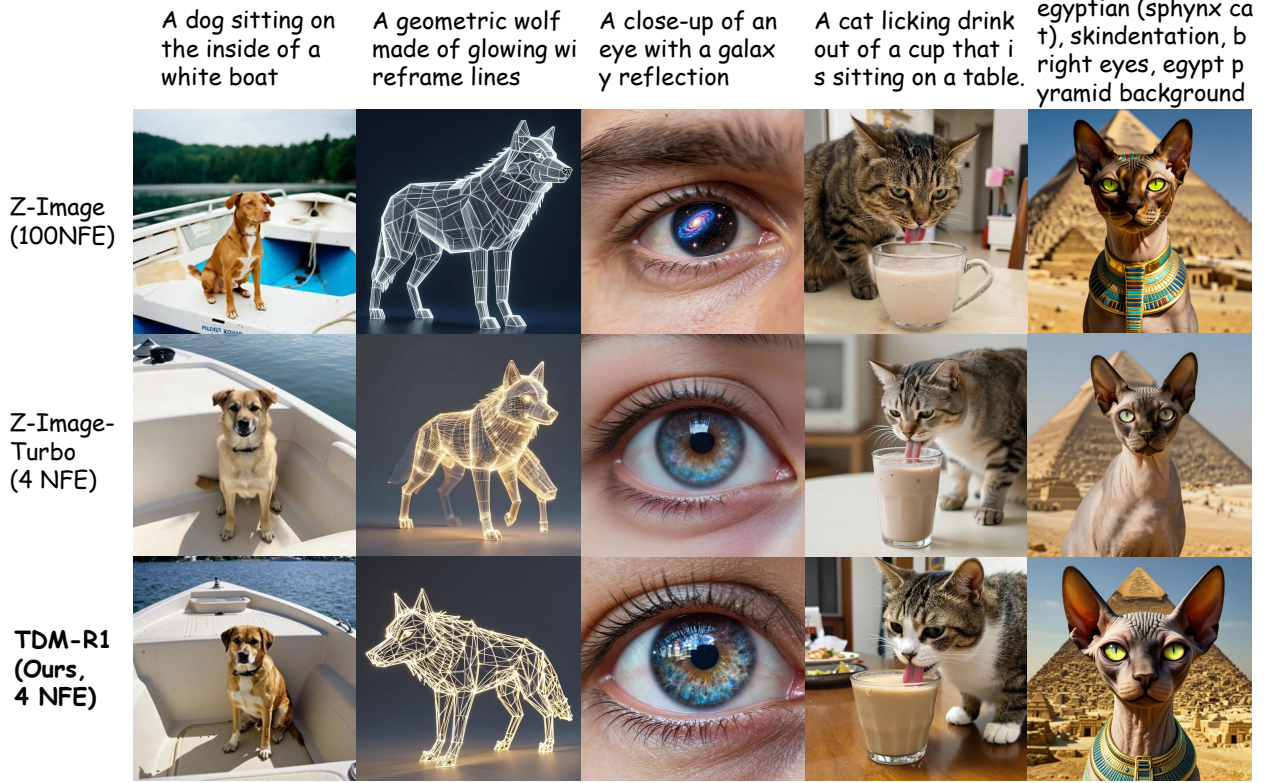


Figure 3 | Qualitative comparisons of TDM-R1 against competing methods.

Trajectory Distribution Matching (TDM). TDM (Luo et al., 2025c) aligns the student trajectory and teacher trajectory at the distributional level. The learning is performed by minimizing the integral reverse KL divergence (Luo et al., 2023; Wang et al., 2023) at each step of the K -step student trajectory as follows:

$$\begin{aligned} \nabla_{\theta} L(\theta) &= \mathbb{E}_{k, t \geq t_k} \lambda_t [\nabla_{\mathbf{x}_t} \text{KL}(p_{\theta, k}(\mathbf{x}_t) \| p_{\psi}(\mathbf{x}_t))] \frac{\partial \mathbf{x}_{t_k}}{\partial \theta} \\ &\approx \mathbb{E}_{k, t \geq t_k, q(\mathbf{x}_t | \mathbf{x}_{t_k})} \lambda_t [s_{\text{fake}}(\mathbf{x}_t) - s_{\psi}(\mathbf{x}_t)] \frac{\partial \mathbf{x}_{t_k}}{\partial \theta}, \end{aligned} \quad (2)$$

where $t_k = \frac{T}{K}k$ by default, T is the terminal timestep, $p_{\theta, k}(\mathbf{x}_t) \triangleq \int q(\mathbf{x}_t | \mathbf{x}_{t_k}) p_{\theta}(\mathbf{x}_{t_k}) d\mathbf{x}_{t_k}$, $p_{\theta}(\mathbf{x}_{t_k})$ is the distribution of student trajectory at timestep t_k , the $p_{\psi}(\mathbf{x}_t)$ is the pre-trained teacher DM, and an online fake score $s_{\text{fake}}(\mathbf{x}_t)$ is employed to approximate the score of student distribution.

Reward Modeling and RLHF. Consider ranked pairs derived from a condition \mathbf{c} denoted $\mathbf{x}_0^w \succ \mathbf{x}_0^l | \mathbf{c}$, where \mathbf{x}_0^w represents the preferred sample and \mathbf{x}_0^l represents the less preferred sample. The Bradley-Terry (BT) model characterizes the pairwise preferences as:

$$p_{\text{BT}}(\mathbf{x}_0^w \succ \mathbf{x}_0^l | \mathbf{c}) = \sigma(r(\mathbf{c}, \mathbf{x}_0^w) - r(\mathbf{c}, \mathbf{x}_0^l)), \quad (3)$$

where $\sigma(\cdot)$ is the sigmoid function. A parameterized reward network r_{ϕ} can then be learned through maximum likelihood estimation: $\min_{\phi} -\log p_{\text{BT}}(\mathbf{x}_0^w \succ \mathbf{x}_0^l | \mathbf{c})$.

The target of RLHF is to optimize a conditional generator $p_{\theta}(\mathbf{x}_0 | \mathbf{c})$ such that it maximizes an certain reward $r_{\phi}(\mathbf{c}, \mathbf{x}_0)$ while remaining close to a reference distribution p_{ref} via:

$$\max_{p_{\theta}} \mathbb{E}_{\mathbf{c}, \mathbf{x}_0 \sim p_{\theta}(\mathbf{x}_0 | \mathbf{c})} [r(\mathbf{c}, \mathbf{x}_0)] - \beta \text{KL} [p_{\theta}(\mathbf{x}_0 | \mathbf{c}) | p_{\text{ref}}(\mathbf{x}_0 | \mathbf{c})]. \quad (4)$$

Here, β controls the strength of the regularization.

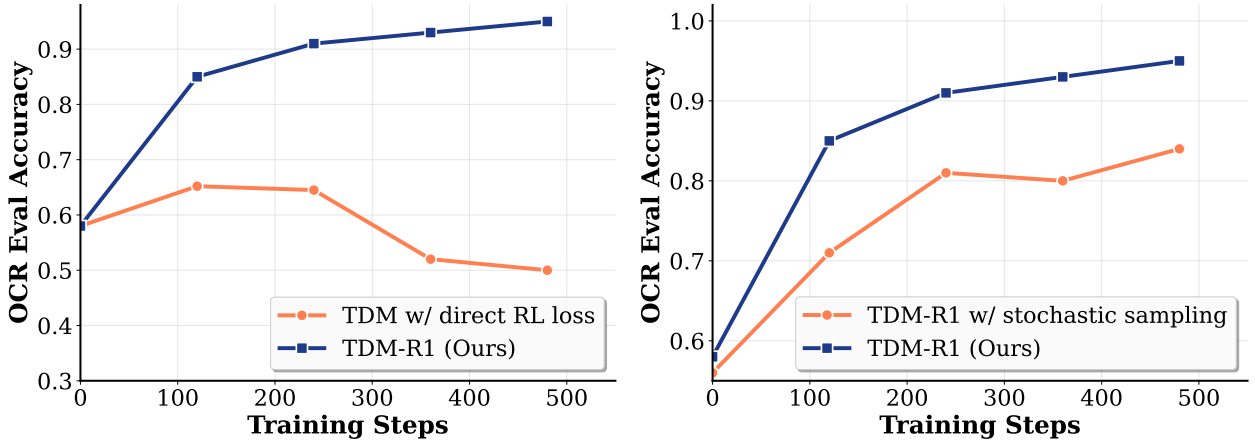


Figure 4 | Compare the training performance and speed of TDM-R1 and potential baselines.

3. Method

Problem Setup. Let p_θ denote a pre-trained few-step diffusion model parameterized by θ . We assume access to a dataset of conditions $\mathcal{D}_c = \{\mathbf{c}_i\}_{i=1}^N$ and a reward function $r(\cdot, \cdot) : \mathcal{X} \times \mathcal{C} \rightarrow \mathbb{R}$ that measures the quality of generated samples $\mathbf{x} \in \mathcal{X}$ with respect to a given condition $\mathbf{c} \in \mathcal{C}$. Our goal is to reinforce the few-step diffusion model p_θ according to the non-differentiable reward signal. We adopt an online RL framework: at each training iteration, the current model p_θ produces a group of samples conditioned on $c \in \mathcal{D}_c$ through K -step sampling. The samples generated along each trajectory are collected into datasets $\mathcal{D}_k = \{(\mathcal{G}_i = \{\mathbf{x}_{t_k, j}\}_{j=1}^G, \mathbf{c}_i) \mid \mathbf{x}_{t_k, j} \sim p_\theta(\cdot, t_k | \mathbf{c}_i)\}$, which are subsequently scored by the reward function to obtain training signals.

Overview. Our method addresses reinforcement learning of few-step diffusion models through three key components. First, in Section 3.1, we establish that deterministic sampling trajectories—as employed by trajectory distribution matching (TDM)—enable accurate reward estimation for intermediate steps (Eq. (7)). Second, in Section 3.2, we address the incompatibility between standard diffusion RL methods and few-step generation by introducing a Surrogate Reward. This module learns a fine-grained, differentiable reward for each step along the trajectory via group-based preference optimization. Third, in Section 3.3, we formulate the learning objective for the few-step generator.

3.1. Accurate Intermediate Reward Estimation via Deterministic Trajectories

In order to leverage reward signals to reinforce a well-trained few-step model. An obvious challenge is that reward signals are generally defined over clean images, while few-step models perform inference by progressively denoising from noise to images, making it difficult to assign rewards to intermediate steps. Previous works often directly use the reward at the endpoint of the sampling trajectory as the reward for the entire diffusion path (Liu et al., 2025; Xue et al., 2025b), which introduces bias into the rewards assigned to intermediate steps. Fortunately, prior works (Luo et al., 2025b) have discovered that a conditional probability over noisy images $p(\mathbf{c} | \mathbf{x}_t)$ can be obtained as follows:

$$p(\mathbf{c} | \mathbf{x}_t) = \int p(\mathbf{c} | \mathbf{x}) p(\mathbf{x} | \mathbf{x}_t) d\mathbf{x}. \quad (5)$$

If we normalize $r(\mathbf{x}, \mathbf{c})$ to $[0, 1]$ and interpret this value as the probability that image \mathbf{x} is a good sample given condition \mathbf{c} , i.e., $p(\text{"x is a good sample"} | \mathbf{x}, \mathbf{c}) = r(\mathbf{x}, \mathbf{c})$, we can model the reward for the noisy image \mathbf{x}_t by:

$$r(\mathbf{x}_t, \mathbf{c}) = \int r(\mathbf{x}, \mathbf{c}) p(\mathbf{x} | \mathbf{x}_t) d\mathbf{x} = \mathbb{E}_{p(\mathbf{x} | \mathbf{x}_t)} r(\mathbf{x}). \quad (6)$$

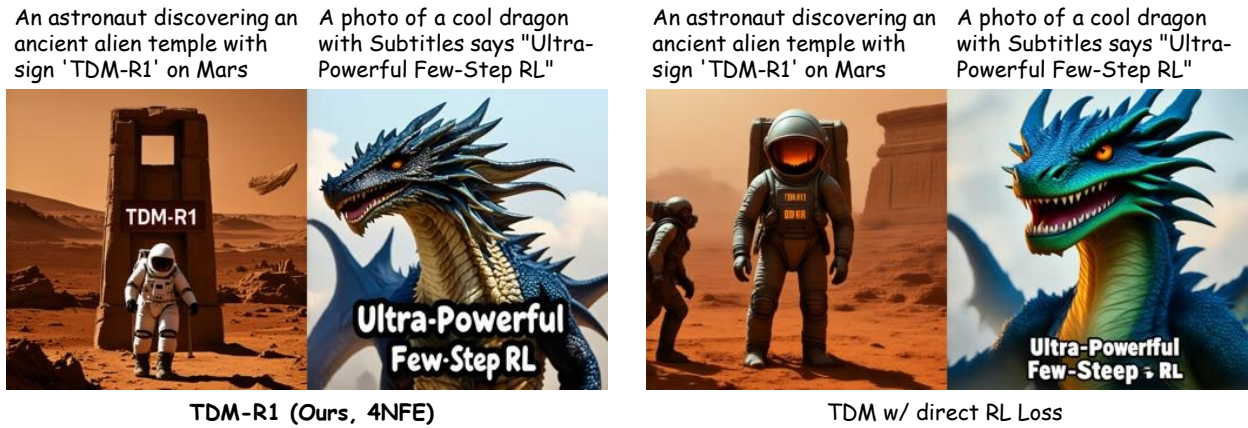


Figure 5 | Compare TDM-R1 with the direct combination of TDM and RL loss.

This Eq. (6) actually justifies the reasonableness of defining the reward for the entire diffusion path using the reward of x_0 , which is a single-sample estimate of the Eq. (6). The variance of this estimate depends on the variance of $p(\mathbf{x}|\mathbf{x}_t)$.

In other words, if $p(\mathbf{x}|\mathbf{x}_t)$ is a deterministic Dirac distribution—i.e., for diffusion, the path from \mathbf{x}_t to x_0 is obtained via ODE sampling – then we can obtain an unbiased estimate of the reward for intermediate samples along the sampling path, which will significantly reduce the variance of reward estimation. This also explains why Mix-GRPO achieves superior performance by converting some SDE steps into ODE steps in RL’s rollout (Li et al., 2026) — it reduces the variance of estimating rewards for intermediate samples along the trajectory.

Through the above analysis, we propose to conduct reinforcement learning based on TDM—a state-of-the-art few-step diffusion model that performs sampling through deterministic trajectories, allowing us to obtain accurate reward estimates for every intermediate sample along the trajectory, thereby achieving superior reinforcement post-training. Compared with the stochastic trajectories, the deterministic trajectories enable more accurate reward estimation for intermediate step, leading to faster convergence and better ultimate performance (Fig. 4).

3.2. Surrogate Reward Learning

Given non-differentiable reward signals and a well-trained few-step diffusion model, a natural idea is to directly apply RL methods designed for standard diffusion models to few-step diffusion models. While this approach can leverage reward signals to some extent, it fails to sufficiently improve performance or generate high-quality images—outputs tend to be blurry, as shown in Figs. 4 and 5. This is because RL methods for standard diffusion models that handle non-differentiable rewards can typically be reformulated as, or are equivalent to, weighted combinations of denoising losses (Wallace et al., 2024; Xue et al., 2025a; Zheng et al., 2025). Due to the inherent characteristics of denoising losses, they tend to produce blurry results with few sampling steps, making them incompatible with few-step diffusion models (Luo et al., 2025b).

To more effectively leverage non-differentiable reward signals, we propose learning a Surrogate Reward for reinforcement and using this Surrogate Reward to guide model learning. Inspired by the success of prior work (Luo et al., 2025d; Wallace et al., 2024), which have demonstrated the effectiveness of parameterizing reward models using the diffusion models, we adopt a similar approach. Specifically, they derive from the RLHF objective that the reward for a clean image \mathbf{x}_0 can

be approximately parameterized as:

$$\tilde{r}_\phi(\mathbf{x}_0, \mathbf{c}) \approx \beta \mathbb{E}_{q(\mathbf{x}_{1:T}|\mathbf{x}_0)} \log \frac{p_\theta(\mathbf{x}_{0:T}|\mathbf{c})}{p_{\text{ref}}(\mathbf{x}_{0:T}|\mathbf{c})} + \beta \log Z(\mathbf{c}).$$

Through a similar derivation, we can parameterize the surrogate reward for a noisy sample \mathbf{x}_{t_k} as follows:

$$\tilde{r}_\phi(\mathbf{x}_{t_k}, \mathbf{c}) \approx \beta \mathbb{E}_{q(\mathbf{x}_{t_k+1:T}|\mathbf{x}_{t_k})} \log \frac{p_\phi(\mathbf{x}_{t_k:T}|\mathbf{c})}{p_{\text{ref}}(\mathbf{x}_{t_k:T}|\mathbf{c})} + \beta \log Z(\mathbf{c}). \quad (7)$$

One could learn this Surrogate Reward through preference relations between pairwise positive and negative samples. However, this approach cannot leverage fine-grained rewards and relative preference relations within groups, limiting the effectiveness of reward learning. In contrast, group-based methods have achieved widespread success in both the language models and image generation (DeepSeek-AI, 2025; Liu et al., 2025).

Therefore, we propose directly learning preference relations between pairwise positive and negative groups of noisy samples using the Bradley-Terry (BT) model. Following prior work (Luo et al., 2025d), we formulate the learning objective as follows:

$$\min -\log p(\mathcal{G}_k^+ \succ \mathcal{G}_k^- | \mathbf{c}) = -\log \frac{1}{1 + \exp(R(\mathcal{G}_k^-) - R(\mathcal{G}_k^+))}, \quad (8)$$

where $\mathcal{G}_k^+ \cup \mathcal{G}_k^- = \mathcal{G}_k$, and the group-level reward $R(\mathcal{G})$ is defined as the weighted sum of rewards for each sample within the group, i.e., $R(\mathcal{G}_k) = \sum_{\mathbf{x} \in \mathcal{G}_k} \omega(\mathbf{x}_{t_k}) \tilde{r}_\phi(\mathbf{x}_{t_k}, \mathbf{c})$.

The weight $\omega(\mathbf{x}_{t_k})$ controls the importance level of each noisy sample within the group, which is set to the absolute normalized value of the advantage within the group, i.e., $\omega(\mathbf{x}_{t_k}^i) = |A(\mathbf{x}_{t_k}^i)| = \left| \frac{r_i - \text{mean}(\{r_j\}_{j=1}^G)}{\text{std}(\{r_j\}_{j=1}^G)} \right|$. This design assigns larger weights to samples that are either significantly better or worse within the group, providing fine-grained learning signals.

The partition into positive and negative groups is based on the advantage $A(\mathbf{x}_{t_k}^i)$, i.e.,

$$\mathcal{G}_k^+ = \{\mathbf{x}_{t_k}^i : A(\mathbf{x}_{t_k}^i) > 0\}, \quad \mathcal{G}_k^- = \{\mathbf{x}_{t_k}^i : A(\mathbf{x}_{t_k}^i) \leq 0\}.$$

Through some calculation, a tractable upper-bound of loss in Eq. (8) can be rewritten in the following form:

$$L(\theta) \leq \mathbb{E}_{(\mathcal{G}_k^+, \mathcal{G}_k^-) \sim \mathcal{D}_{k,k}} \mathbb{E}_{t \geq t_k, q(\mathbf{x}_t | \mathbf{x}_{t_k})} \log \sigma(-\beta(T - t_k) \{ \sum_{\mathbf{x}_{t_k} \in \mathcal{G}_k^+} \omega(\mathbf{x}_{t_k}) [\Delta \text{KL}_\phi(\mathbf{x}_t, \mathbf{x}_{t_k}) - \sum_{\mathbf{x}_{t_k} \in \mathcal{G}_k^-} \omega(\mathbf{x}_{t_k}) \cdot [\Delta \text{KL}_\phi(\mathbf{x}_t, \mathbf{x}_{t_k})]] \}), \quad (9)$$

where

$$\Delta \text{KL}_\phi(\mathbf{x}_t, \mathbf{x}_{t_k}) \triangleq \text{KL}(q(\mathbf{x}_{t-1} | \mathbf{x}_t, \mathbf{x}_{t_k}) || p_\phi(\mathbf{x}_{t-1} | \mathbf{x}_t)) - \text{KL}(q(\mathbf{x}_{t-1} | \mathbf{x}_t, \mathbf{x}_{t_k}) || p_{\text{ref}}(\mathbf{x}_{t-1} | \mathbf{x}_t)).$$

In Eq. (9), we omitted the condition \mathbf{c} for simplicity without loss of generality. Derivations are deferred in Appendix A. Under the Gaussian parameterization (Song et al., 2020), the posterior and model distributions are given by: $q(\mathbf{x}_{t-1} | \mathbf{x}_t, \mathbf{x}_{t_k}) \triangleq \mathcal{N}(\alpha_{t|t_k} \mathbf{x}_{t_k} + \sqrt{\sigma_{t-1|t_k}^2 - \eta_t^2} \epsilon, \eta_t^2 I)$ and $p_\phi(\mathbf{x}_{t-1} | \mathbf{x}_t) \triangleq \mathcal{N}(\alpha_{t-1} \frac{\mathbf{x}_t - \sigma_t \epsilon_\phi}{\alpha_t} + \sqrt{\sigma_t^2 - \eta_t^2} \epsilon_\phi, \eta_t^2 I)$.

Dynamic Reference Model. A frozen reference model may impose overly strong regularization, thereby hindering the learning of the reward model. Prior work has opted to update the reference model with theta at fixed intervals. However, this approach may introduce instability: θ might overfit

Algorithm 1 TDM-R1

Require: Few-step diffusion model p_θ , surrogate reward model \tilde{r}_ϕ , reward function r , group size G , number of iterations N , number of denoising steps K .

Ensure: Reinforced few-step model p_θ .

- 1: **for** $n \leftarrow 1$ **to** N **do**
- 2: // Sample conditioning and generate group
- 3: Sample conditioning $\mathbf{c} \sim \mathcal{D}_c$
- 4: Generate group $\mathcal{G} = \{\mathbf{x}_0^{(1)}, \dots, \mathbf{x}_0^{(G)}\}$ by sampling from $p_{\theta^-}(\cdot | \mathbf{c})$ with K steps
- 5: // Access reward feedback
- 6: Compute rewards: $r_i \leftarrow r(\mathbf{c}, \mathbf{x}_0^{(i)})$ for $i = 1, \dots, G$
- 7: // Update models
- 8: Update surrogate reward \tilde{r}_ϕ via Eq. (9)
- 9: Update fake score s_{fake} via denoising on perturbed generated samples (Eq. (1)).
- 10: Update few-step generator p_θ via Eq. (10)

to noisy signals at a certain step and subsequently be used as the reference model. To achieve better dynamic updating of the reference model, we propose to use an EMA (Exponential Moving Average) version of ϕ as the reference model. This not only relaxes the regularization to facilitate better reward learning, but also mitigates the risk of adopting a “bad” reference model that has overfitted to noisy signals.

3.3. Few-Step Generator Learning

We formulate the reinforcement learning training objective for the K -step generator in a form similar to standard RLHF (Luo et al., 2023, 2024b), consisting of reward maximization with a reverse KL regularization as follows:

$$L(\theta) = \mathbb{E}_{k, p_\theta(\mathbf{x}_{t_k})} - \tilde{r}_{\text{sg}(\phi)}(\mathbf{x}_{t_k}, \mathbf{c}) + \beta_g \text{KL}(p_{\theta, k}(\mathbf{x}_t) || p_\psi(\mathbf{x}_t)), \quad (10)$$

where $p_{\theta, k}(\mathbf{x}_t) \triangleq \int q(\mathbf{x}_t | \mathbf{x}_{t_k}) p_\theta(\mathbf{x}_{t_k}) d\mathbf{x}_{t_k}$. In the objectives described above, Surrogate Reward maximization provides a good learning signal to integrate non-differentiable reward feedback, while the marginal-level reverse KL regularization effectively grounds the generated samples to the base distribution parameterized by the pretrained diffusion model at the distribution level. This differs from the KL regularization adopted in standard diffusion RL (Fan et al., 2024; Liu et al., 2025), which is essentially an instance-level constraint that requires each point along the trajectory to be consistent with the base model, leading to an unnecessarily difficult constraint.

Put the reward parameterization in Eq. (7) into Eq. (10), we can derive the learning gradient with some calculations as follows:

$$\begin{aligned} \nabla_\theta L(\theta) = & -\mathbb{E}_{k, t \geq t_k} \mathbb{E}_{p_\theta(\mathbf{x}_{t_k})} \mathbb{E}_{q(\mathbf{x}_t, \mathbf{x}_{t-1} | \mathbf{x}_{t_k})} \left[\beta \alpha_{t|t_k} (T - t_k) \nabla_{\mathbf{x}_t} \log \frac{p_\phi(\mathbf{x}_{t-1} | \mathbf{x}_t)}{p_{\text{ref}}(\mathbf{x}_{t-1} | \mathbf{x}_t)} \right. \\ & \left. + \beta_g \lambda_t (s_{\text{fake}}(\mathbf{x}_t) - s_\psi(\mathbf{x}_t)) \right] \frac{\partial \mathbf{x}_{t_k}}{\partial \theta}, \end{aligned} \quad (11)$$

where we stop the gradient of ϕ to save the memory cost, and we found that it does not affect the performance. We defer the derivation to Appendix A. Following standard practice (Luo et al., 2023, 2024a, 2025c; Yin et al., 2023; Zhou et al., 2024), we adopt an online fake score s_{fake} for estimating the score of student distribution, which is trained by denoising score matching.

Table 1 | **GenEval Result.** We **highlight** the best scores among specific category. Obj.: Object; Attr.: Attribution.

Model	Overall	Single Obj.	Two Obj.	Counting	Colors	Position	Attr. Binding
<i>Autoregressive Models:</i>							
Show-o (Xie et al., 2024a)	0.53	0.95	0.52	0.49	0.82	0.11	0.28
Emu3-Gen (Wang et al., 2024)	0.54	0.98	0.71	0.34	0.81	0.17	0.21
JanusFlow (Ma et al., 2025)	0.63	0.97	0.59	0.45	0.83	0.53	0.42
Janus-Pro-7B (Chen et al., 2025)	0.80	0.99	0.89	0.59	0.90	0.79	0.66
GPT-4o (Hurst et al., 2024)	0.84	0.99	0.92	0.85	0.92	0.75	0.61
<i>Diffusion Models:</i>							
LDM (Rombach et al., 2022)	0.37	0.92	0.29	0.23	0.70	0.02	0.05
SD1.5 (Rombach et al., 2022)	0.43	0.97	0.38	0.35	0.76	0.04	0.06
SD2.1 (Rombach et al., 2022)	0.50	0.98	0.51	0.44	0.85	0.07	0.17
SD-XL (Podell et al., 2023)	0.55	0.98	0.74	0.39	0.85	0.15	0.23
DALLE-2 (OpenAI, 2023)	0.52	0.94	0.66	0.49	0.77	0.10	0.19
DALLE-3 (Betker et al., 2023)	0.67	0.96	0.87	0.47	0.83	0.43	0.45
FLUX.1 Dev (Labs, 2024)	0.66	0.98	0.81	0.74	0.79	0.22	0.45
SD3.5-L (Esser et al., 2024)	0.71	0.98	0.89	0.73	0.83	0.34	0.47
SANA-1.5 4.8B (Xie et al., 2025)	0.81	0.99	0.93	0.86	0.84	0.59	0.65
SD3.5-M (Esser et al., 2024)	0.63	0.98	0.78	0.50	0.81	0.24	0.52
w/ Flow-GRPO (Liu et al., 2025)	0.95	1.00	0.99	0.95	0.92	0.99	0.86
w/ DGPO (Luo et al., 2025d)	0.97	1.00	0.99	0.97	0.95	0.99	0.91
<i>Few-Step Diffusion Models:</i>							
SD3.5-L-Turbo (4NFE) (Esser et al., 2024)	0.70	0.94	0.84	0.55	0.79	0.58	0.56
TDM-SD3.5-M (4NFE) (Luo et al., 2025c)	0.61	0.99	0.77	0.49	0.79	0.23	0.44
SD3.5-M w/ TDM-R1 (Ours, 4NFE)	0.92	1.00	0.96	0.88	0.85	0.93	0.91

Remark. By joint training of the Few-Step Generator and Surrogate Reward, which establishes a synergistic loop: the Generator progressively produces higher-quality samples via maximize the Surrogate Reward, while the Surrogate Reward adapts to provide increasingly precise guidance by identifying favorable and unfavorable regions at each intermediate step per iteration. This Adaptive Surrogate Reward mechanism implements a GAN-like adversarial framework on self-generated samples, ultimately enabling effective reinforcement post-training for few-step diffusion models with superior generation performance.

In summary, TDM-R1 enables the utilization of large-scale online non-differentiable reward feedback, achieving effective reinforcement post-training for few-step generators. Starting from a pre-trained few-step generator based on Trajectory Distribution Matching (TDM), we alternately optimize the few-step generator to maximize the surrogate reward and minimize the reverse KL divergence, while the surrogate reward is trained through group preference optimization, and the fake score is optimized via the denoising matching objective. See Algorithm 1 for pseudo algorithm.

4. Experiments

This section provides a comprehensive evaluation of TDM-R1. We primarily benchmark performance on two verifiable tasks with non-differentiable metrics: compositional image generation and visual text rendering (Tables 1 and 2). Qualitative comparisons are shown in Fig. 6, and we demonstrate the method’s effectiveness in aligning with human preferences (Fig. 7). Additionally, we ablate key components of our approach (Figs. 4 and 8).

4.1. Experimental Setup

Evaluation Tasks. We begin by pre-training the few-step TDM on SD3.5-M (Esser et al., 2024; Luo et al., 2025c), followed by evaluating our proposed TDM-R1’s effectiveness in reinforcing the

Table 2 | **Performance on Compositional Image Generation and Visual Text Rendering Benchmarks.** ImgRwd: ImageReward; UniRwd: UnifiedReward. We highlight the metric adopted for the training signal. † Results are taken from the original paper.

Model	NFE	Verifiable Metric		Image Quality		Preference Score		
		GenEval	OCR Acc.	Aesthetic	DeQA	ImgRwd	PickScore	UniRwd
SD3.5-M (Esser et al., 2024)	80	0.63	0.59	5.39	4.07	0.87	22.34	3.33
Flow-GRPO† (Liu et al., 2025)	80	0.95	—	5.25	4.01	1.03	22.37	3.51
DGPO† (Luo et al., 2025d)	80	0.97	—	5.31	4.03	1.08	22.41	3.60
Flow-GRPO† (Liu et al., 2025)	80	—	0.92	5.32	4.06	0.95	22.44	3.42
DGPO† (Luo et al., 2025d)	80	—	0.96	5.37	4.09	1.02	22.52	3.48
TDM-SD3.5-M (Luo et al., 2025c)	4	0.61	0.55	5.41	4.05	0.99	22.36	3.30
<i>Compositional Image Generation:</i>								
p_ϕ in Surrogate Reward	80	0.89	0.52	5.35	4.01	0.94	22.31	3.48
TDM-R1 (Ours)	4	0.92	0.59	5.42	4.07	1.11	22.39	3.55
<i>Visual Text Rendering:</i>								
p_ϕ in Surrogate Reward	80	0.64	0.92	5.41	4.05	0.98	22.37	3.43
TDM-R1 (Ours)	4	0.67	0.95	5.45	4.11	1.09	22.62	3.51

Table 3 | **Performance on reinforcing Z-Image.** ImgRwd: ImageReward; UniRwd: UnifiedReward. We highlight the metric adopted for the training signal.

Model	NFE	Verifiable Metric		Model-based Metric				
		GenEval	OCR Acc.	HPSv3	Aesthetic	ImgRwd	PickScore	UniRwd
Z-Image	100	0.66	0.74	7.32	5.35	0.62	19.98	3.64
Z-Image-Turbo (DMDR)	4	0.73	0.78	9.13	5.40	0.78	20.28	3.70
TDM-R1-Zimage (Ours)	4	0.77	0.79	9.90	5.49	0.94	20.45	3.75

TDM-SD3.5-M across two valuable tasks with verifiable metrics: 1) *Compositional Image Generation*: assessed using GenEval (Ghosh et al., 2023), which encompasses six demanding compositional generation scenarios, including object counting, spatial relationships, and attribute binding; 2) *Visual Text Rendering*: measures the model’s capability to accurately synthesize text within generated images (Gong et al., 2025).

Out-of-Domain Evaluation Metrics. To ensure fair assessment and mitigate reward hacking—a phenomenon where models overfit to training reward signals at the expense of actual image quality—we utilize five independent image quality metrics excluded from training as out-of-domain evaluations: Aesthetic Score (Schuhmann et al., 2022), DeQA (You et al., 2025), ImageReward (Xu et al., 2023), PickScore (Kirstain et al., 2023), and UnifiedReward (Wang et al., 2025a). These metrics are computed on DrawBench (Saharia et al., 2022), a comprehensive benchmark comprising diverse prompts.

4.2. Main Results

Quantitative Results. Table 1 shows that our proposed TDM-R1 achieves competitive performance on GenEval, notably surpassing prior commercial closed-source SOTA GPT-4o and matches the performance of prior SOTA standard diffusion RL. *This promising performance is achieved while also showing improvement across various out-of-domain metrics (such as AeS, DeQA, PickScore, and Image Reward), as indicated by Table 2.* It is worth noting that, although previous SOTA of standard diffusion RL (e.g., Flow-GRPO and DGPO) achieved higher GenEval scores, they exhibited noticeable

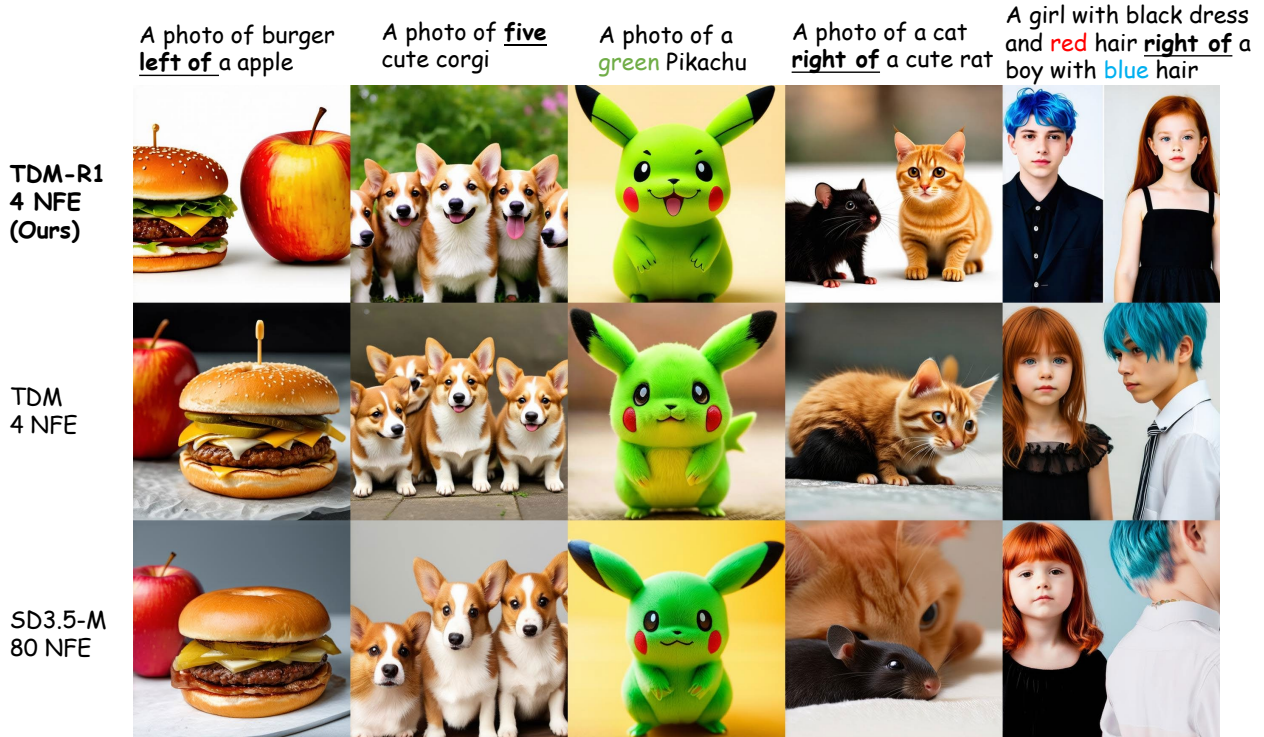


Figure 6 | Qualitative comparisons of TDM-R1 with GenEval signals against competing methods. It can be seen that our proposed TDM-R1 can accurately follow the instructions, while keeping a strong visual quality. The same initial noise is used to generate all images.

degradation in metrics measuring image quality. In contrast, our TDM-R1 even achieves higher image quality metrics compared to both the many-step base model and the few-step base model.

Beyond compositional image generation, Table 2 provides detailed evaluation results on visual text rendering, where DGPO similarly demonstrates significant improvements in both target optimization metrics and out-of-domain metrics. *Notably, we found that training on a verifiable metric (GenEval score or OCR score) can synergistically improve a completely different verifiable metric.* This is a surprising and encouraging signal, suggesting that we may be able to enhance the broad instruction-following capabilities of few-step diffusion models through a well-chosen proxy task.

Qualitative Comparison. We present qualitative results from our method and baselines, trained with GenEval’s signal, in Fig. 6. The visualizations demonstrate that TDM-R1 follows instructions more accurately than both the few-step baseline and the 80-NFE base model, while preserving high generation quality. See Appendix C for additional visual samples.

Human Preference Alignment. We also evaluate TDM-R1 on Human Preference Alignment. In this task, we employ ImageReward (Xu et al., 2023) and HPS (Wu et al., 2023) as the reward signal separately. Although these metrics are differentiable, we do not use their gradient. Both HPS and ImageReward are trained on large-scale human preference data, providing a comprehensive assessment of generation quality from a human-centric perspective. As shown in Fig. 7, our proposed TDM-R1 can effectively enhance the performance of few-step models with these metrics that evaluate human preference.

Human Preference Alignment on Large Model. We further evaluate TDM-R1 on aligning a larger model, the recent and powerful open-source Z-Image (Team et al., 2025) with 6B parameters, using HPSv3 as the reward signal. HPSv3 is a state-of-the-art reward model that serves as a robust metric for

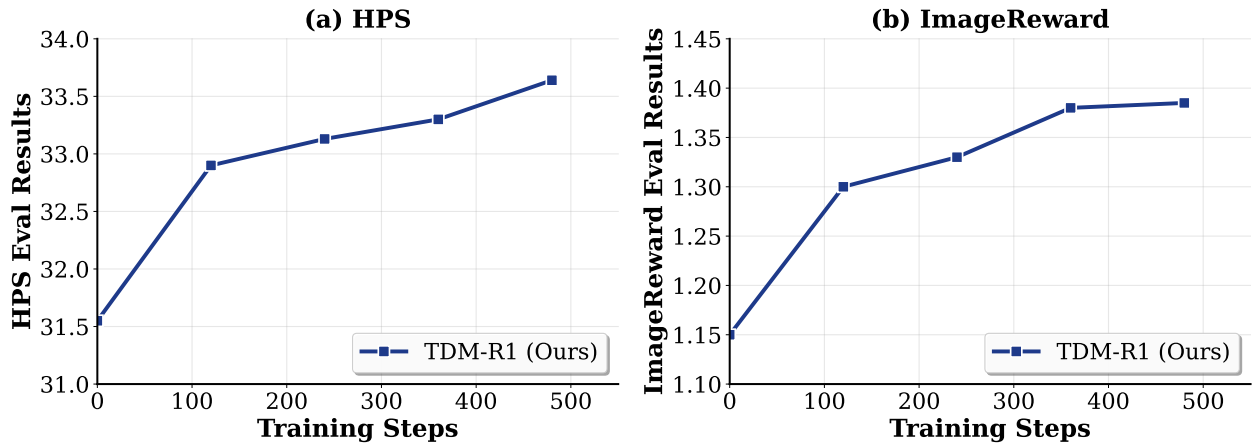


Figure 7 | TDM-R1 Performance in human preference alignment.

wide-spectrum image evaluation. As shown in Table 3, TDM-R1 effectively enhances the performance of Z-Image across both in-domain and out-of-domain metrics, notably outperforming the many-step Z-Image and the few-step Z-Image-Turbo. We also provide visual comparisons against competing methods in Fig. 3, demonstrating consistent improvement over the baselines

Comparison with the Surrogate Reward Model. Since our Surrogate Reward is parameterized by a diffusion model p_ϕ , an interesting experimental question arises: how does the performance of the diffusion model p_ϕ that parameterizes this reward compare to our few-step generator TDM-R1? As shown in Table 2, p_ϕ achieves substantially better task metrics than the base model. Notably, however, TDM-R1—which requires only 4 NFE for sampling—consistently outperforms p_ϕ (which requires 80 NFE) on both in-domain and out-of-domain metrics. This result may appear counterintuitive, given that TDM-R1 is trained using signals derived from the very Surrogate Reward parameterized by p_ϕ . Yet this observation aligns with findings from the LLM literature on DPO-like methods: improving a model’s performance as a reward signal does not necessarily translate to improved generation performance in inference. The key insight is that effective training of TDM-R1 depends not on p_ϕ ’s generation capabilities, but rather on the quality of the reward signal it provides. These results demonstrate that our Surrogate Reward has been effectively tailored as a per-step reward model, enabling superior reinforcement fine-tuning performance for TDM-R1.

4.3. Ablation Study

TDM-R1 v.s. Direct RL Loss Combination. A fairly straightforward and natural baseline is to directly combine the distillation loss with an RL loss designed for standard diffusion models to reinforce the few-step generator. We adopt DGPO (Luo et al., 2025d), a recent state-of-the-art RL method for diffusion models, as the accompanying RL loss and combine it with TDM’s distillation loss as a potential baseline, termed TDM w/ direct RL loss. As shown in Figs. 4 and 5, while this baseline achieves modest performance improvements in the early stages (though still far inferior to TDM-R1), it produces blurry images and suffers from performance degradation in later training stages. This decline in image quality stems from a fundamental mismatch: the denoising objective inherent in standard diffusion RL is incompatible with reverse KL divergence minimization in distillation, as the direct denoising behavior enforced by RL loss may be suboptimal for few-step generation.

Dynamic Surrogate Reward v.s. Frozen Well-Trained Reward. Our proposed TDM-R1 jointly trains the Dynamic Surrogate Reward and the few-step generator throughout the training process. We compared this approach against a notable baseline: directly using the reward model trained by DGPO. This baseline can be viewed as using an RL-trained diffusion model as a teacher to distill a

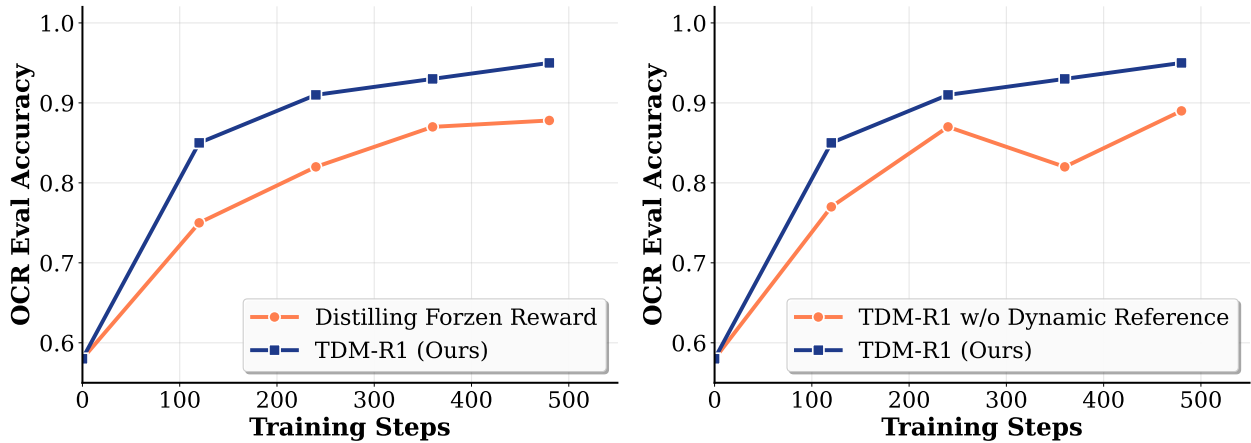


Figure 8 | Comparison of visual text alignment across variants.

few-step student. As shown in Fig. 8, the Dynamic Surrogate Reward achieves faster reward growth and superior final performance compared to distillation with a frozen reward. We attribute this improvement to two factors. First, the Dynamic Surrogate Reward can dynamically identify regions where the few-step student performs well or poorly, enabling more targeted optimization—a capability that the frozen reward lacks. Second, a distribution gap exists between the few-step generator’s outputs and the data distribution on which the frozen reward was originally trained, which can lead to suboptimal guidance and degraded performance.

Comparison with Distilled RL Diffusion. We also compare TDM-R1 against a competitive baseline: initializing with an RL-finetuned diffusion model (i.e., DGPO) followed by distillation via TDM. As shown in Fig. 9, TDM initialized with DGPO converges quickly in the early stages, but its performance ceiling is constrained by the teacher model, causing it to plateau rapidly. In contrast, TDM-R1 continuously incorporates reward signals throughout training, ultimately achieving superior performance. Although this baseline is beyond our scope — our goal is to directly post-train few-step diffusion models rather than first training a teacher and then distilling a few-step student, which introduces additional pipeline complexity — this ablation clearly demonstrates that *TDM-R1 is not only more elegant as a paradigm, directly reinforcing the well-trained few-step student model, but also achieves stronger final performance.*

Effect of the Deterministic Path. A core feature of our method is its ability to leverage deterministic trajectories for step-by-step reward feedback. While stochastic trajectories can theoretically achieve the same goal, they introduce greater variance in the feedback signal. To evaluate this trade-off, we compared our approach against a variant using stochastic sampling, termed TDM-R1 w/ stochastic sampling. As shown in Fig. 4, deterministic trajectories yield faster convergence and superior performance.

Effect of the Dynamic Reference Model. We propose using an EMA of p_ϕ as the reference model during surrogate reward learning. This dynamic reference model enables effective optimization. Our experiments confirm the effectiveness of this design: as shown in Figure 8, replacing the dynamic reference model with a static one results in degraded performance and reduced training stability.

5. Related Works

Few-Step Text-to-Image Diffusion Sampling. Although training-free methods for accelerating diffusion model sampling have progressed substantially (Li et al., 2025; Lu et al., 2022; Ma et al., 2024; Si et al., 2024; Xue et al., 2024; Zhao et al., 2023), diffusion distillation (Luo, 2023) remains

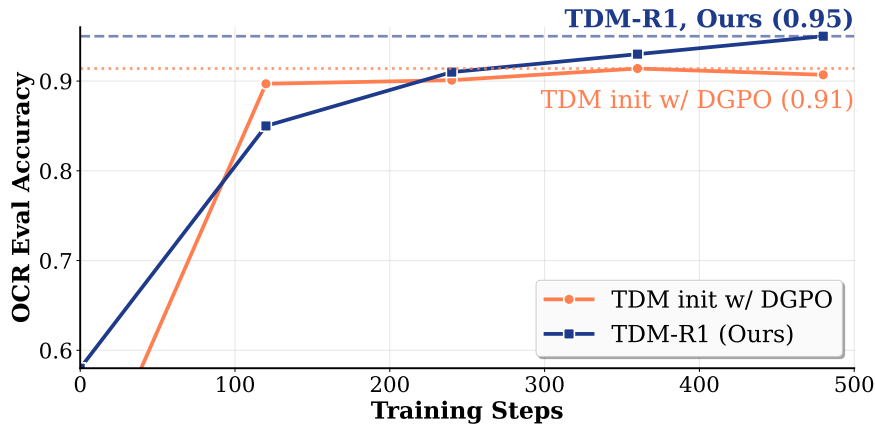


Figure 9 | Comparison between TDM-R1 with direct distillation.

essential for high-quality few-step generation. In general, distilled models perform one or a few more transformations that map random noise to images. The most widely adopted distillation strategies for few-step diffusion sampling fall into two categories: trajectory matching (Geng et al., 2024; Kim et al., 2023; Salimans et al., 2024; Song and Dhariwal; Song et al., 2023) and distribution matching (Luo et al., 2023, 2024a,c; Sauer et al., 2023; Wang et al., 2025b; Xu et al., 2024; Yin et al., 2023; Zhou et al., 2024). More recently, trajectory distribution matching (TDM) (Luo et al., 2025c) has demonstrated strong few-step performance.

Text-Image Alignment. Among the many efforts to improve text-image alignment (Bansal et al., 2023; Ho and Salimans, 2022; Liu et al., 2024; Luo et al., 2025e; Ma et al., 2023), reinforcement learning has emerged as a particularly promising approach. Recent efforts to improve diffusion models through reinforcement learning have explored three main strategies. The first fine-tunes diffusion on high-quality image-prompt pairs (Dai et al., 2023; Podell et al., 2023). The second optimizes explicit rewards, either by evaluating the final outputs of multi-step synthesis (Clark et al., 2023; Ho et al., 2022; Lee et al., 2023; Luo et al., 2025a,b; Prabhudesai et al., 2023) or through policy gradient methods (Black et al., 2023; Fan et al., 2024; Ye et al., 2024). The third bypasses explicit rewards entirely, instead learning directly from preference data, as in Diffusion-DPO (Wallace et al., 2024) and Diffusion-KTO (Yang et al., 2024). More recently, GRPO has been successfully adapted to diffusion models (Liu et al., 2025; Luo et al., 2025d; Xue et al., 2025b), showing strong scalability and notable performance gains. Nevertheless, all these approaches target standard diffusion models. Our work tackles a distinct problem: reinforcing the few-step diffusion models.

Few-Step Text-to-Image Diffusion RL. As for few-step generative models, recent work (Li et al., 2024; Luo, 2024; Luo et al., 2024b, 2025a; Ren et al., 2024) has introduced methods for training preference-aligned few-step text-to-image models, achieving promising results. Nevertheless, these existing approaches for few-step models are restricted to differentiable reward functions, with narrow applications in cases of non-differentiable rewards. Some others theoretically support non-differentiable rewards (Jiang et al., 2025; Miao et al., 2025) by combining standard RL methods, but they have not validated their effectiveness at scales. Furthermore, applying standard RL methods of diffusion models to few-step models would lead to blurry generation and suboptimal performance, as illustrated in Figs. 4 and 5. To our best knowledge, our TDM-R1 is the first work tackling RL with non-differentiable rewards for few-step text-to-image generative models at scales.

6. Conclusion

In this paper, we introduced TDM-R1, a novel reinforcement learning paradigm that enables few-step diffusion models to effectively leverage non-differentiable reward feedback. By building upon Trajectory Distribution Matching and decoupling the learning process into surrogate reward learning and generator optimization, TDM-R1 addresses a fundamental limitation of existing approaches that rely exclusively on differentiable reward signals. Our extensive experiments demonstrate that TDM-R1 consistently achieves state-of-the-art reinforcement learning performance for few-step text-to-image models. Most notably, TDM-R1 enables 4-step models to surpass their expensive 80-NFE base counterparts, with improvements on GenEval from 61% to 92%—exceeding both the 80-NFE base model at 63%. These results validate that few-step diffusion models can successfully incorporate large-scale online non-differentiable reward signals without requiring additional ground-truth image data.

References

- Yuntao Bai, Andy Jones, Kamal Ndousse, Amanda Askell, Anna Chen, Nova DasSarma, Dawn Drain, Stanislav Fort, Deep Ganguli, Tom Henighan, et al. Training a helpful and harmless assistant with reinforcement learning from human feedback. *arXiv preprint arXiv:2204.05862*, 2022.
- Arpit Bansal, Hong-Min Chu, Avi Schwarzschild, Soumyadip Sengupta, Micah Goldblum, Jonas Geiping, and Tom Goldstein. Universal guidance for diffusion models. In *Proceedings of the IEEE/CVF Conference on Computer Vision and Pattern Recognition*, pages 843–852, 2023.
- James Betker, Gabriel Goh, Li Jing, Tim Brooks, Jianfeng Wang, Linjie Li, Long Ouyang, Juntang Zhuang, Joyce Lee, Yufe i Guo, et al. Improving image generation with better captions. *Computer Science*. <https://cdn.openai.com/papers/dall-e-3.pdf>, 2023.
- Kevin Black, Michael Janner, Yilun Du, Ilya Kostrikov, and Sergey Levine. Training diffusion models with reinforcement learning. *arXiv preprint arXiv:2305.13301*, 2023.
- Huanqia Cai, Sihan Cao, Ruoyi Du, Peng Gao, Steven Hoi, Zhaohui Hou, Shijie Huang, Dengyang Jiang, Xin Jin, Liangchen Li, et al. Z-image: An efficient image generation foundation model with single-stream diffusion transformer. *arXiv preprint arXiv:2511.22699*, 2025.
- Jingye Chen, Yupan Huang, Tengchao Lv, Lei Cui, Qifeng Chen, and Furu Wei. Textdiffuser: Diffusion models as text painters. *Advances in Neural Information Processing Systems*, 36:9353–9387, 2023.
- Xiaokang Chen, Zhiyu Wu, Xingchao Liu, Zizheng Pan, Wen Liu, Zhenda Xie, Xingkai Yu, and Chong Ruan. Janus-pro: Unified multimodal understanding and generation with data and model scaling. *arXiv preprint arXiv:2501.17811*, 2025.
- Kevin Clark, Paul Vicol, Kevin Swersky, and David J Fleet. Directly fine-tuning diffusion models on differentiable rewards. *arXiv preprint arXiv:2309.17400*, 2023.
- Xiaoliang Dai, Ji Hou, Chih-Yao Ma, Sam Tsai, Jialiang Wang, Rui Wang, Peizhao Zhang, Simon Vandenhende, Xiaofang Wang, Abhimanyu Dubey, et al. Emu: Enhancing image generation models using photogenic needles in a haystack. *arXiv preprint arXiv:2309.15807*, 2023.
- DeepSeek-AI. Deepseek-r1: Incentivizing reasoning capability in llms via reinforcement learning, 2025. URL <https://arxiv.org/abs/2501.12948>.
-

- Patrick Esser, Sumith Kulal, Andreas Blattmann, Rahim Entezari, Jonas Müller, Harry Saini, Yam Levi, Dominik Lorenz, Axel Sauer, Frederic Boesel, Dustin Podell, Tim Dockhorn, Zion English, Kyle Lacey, Alex Goodwin, Yannik Marek, and Robin Rombach. Scaling rectified flow transformers for high-resolution image synthesis, 2024. URL <https://arxiv.org/abs/2403.03206>.
- Ying Fan, Olivia Watkins, Yuqing Du, Hao Liu, Moonkyung Ryu, Craig Boutilier, Pieter Abbeel, Mohammad Ghavamzadeh, Kangwook Lee, and Kimin Lee. Reinforcement learning for fine-tuning text-to-image diffusion models. *Advances in Neural Information Processing Systems*, 36, 2024.
- Zhengyang Geng, Ashwini Pokle, William Luo, Justin Lin, and J Zico Kolter. Consistency models made easy. *arXiv preprint arXiv:2406.14548*, 2024.
- Dhruba Ghosh, Hannaneh Hajishirzi, and Ludwig Schmidt. Geneval: An object-focused framework for evaluating text-to-image alignment. *Advances in Neural Information Processing Systems*, 36: 52132–52152, 2023.
- Lixue Gong, Xiaoxia Hou, Fanshi Li, Liang Li, Xiaochen Lian, Fei Liu, Liyang Liu, Wei Liu, Wei Lu, Yichun Shi, et al. Seedream 2.0: A native chinese-english bilingual image generation foundation model. *arXiv preprint arXiv:2503.07703*, 2025.
- Jonathan Ho and Tim Salimans. Classifier-free diffusion guidance. *arXiv preprint arXiv:2207.12598*, 2022.
- Jonathan Ho, Ajay Jain, and Pieter Abbeel. Denoising diffusion probabilistic models. *Advances in Neural Information Processing Systems*, 33:6840–6851, 2020.
- Jonathan Ho, William Chan, Chitwan Saharia, Jay Whang, Ruiqi Gao, Alexey Gritsenko, Diederik P Kingma, Ben Poole, Mohammad Norouzi, David J Fleet, et al. Imagen video: High definition video generation with diffusion models. *arXiv preprint arXiv:2210.02303*, 2022.
- Aaron Hurst, Adam Lerer, Adam P Goucher, Adam Perelman, Aditya Ramesh, Aidan Clark, AJ Ostrow, Akila Welihinda, Alan Hayes, Alec Radford, et al. Gpt-4o system card. *arXiv preprint arXiv:2410.21276*, 2024.
- Dengyang Jiang, Dongyang Liu, Zanyi Wang, Qilong Wu, Liuzhuozheng Li, Hengzhuang Li, Xin Jin, David Liu, Zhen Li, Bo Zhang, Mengmeng Wang, Steven Hoi, Peng Gao, and Harry Yang. Distribution matching distillation meets reinforcement learning, 2025. URL <https://arxiv.org/abs/2511.13649>.
- Dongjun Kim, Chieh-Hsin Lai, Wei-Hsiang Liao, Naoki Murata, Yuhta Takida, Toshimitsu Uesaka, Yutong He, Yuki Mitsufuji, and Stefano Ermon. Consistency trajectory models: Learning probability flow ode trajectory of diffusion. *arXiv preprint arXiv:2310.02279*, 2023.
- Yuval Kirstain, Adam Polyak, Uriel Singer, Shahbuland Matiana, Joe Penna, and Omer Levy. Pick-a-pic: An open dataset of user preferences for text-to-image generation. *Advances in neural information processing systems*, 36:36652–36663, 2023.
- Black Forest Labs. Flux. <https://github.com/black-forest-labs/flux>, 2024.
- Kimin Lee, Hao Liu, Moonkyung Ryu, Olivia Watkins, Yuqing Du, Craig Boutilier, Pieter Abbeel, Mohammad Ghavamzadeh, and Shixiang Shane Gu. Aligning text-to-image models using human feedback. *arXiv preprint arXiv:2302.12192*, 2023.
- Jiachen Li, Weixi Feng, Wenhui Chen, and William Yang Wang. Reward guided latent consistency distillation. *arXiv preprint arXiv:2403.11027*, 2024.
-

- Junzhe Li, Yutao Cui, Tao Huang, Yinpeng Ma, Chun Fan, Miles Yang, and Zhao Zhong. Mixgrpo: Unlocking flow-based grpo efficiency with mixed ode-sde, 2026. URL <https://arxiv.org/abs/2507.21802>.
- Tiancheng Li, Weijian Luo, Zhiyang Chen, Liyuan Ma, and Guo-Jun Qi. Self-guidance: Boosting flow and diffusion generation on their own. *IEEE Transactions on Pattern Analysis and Machine Intelligence*, 2025.
- Jie Liu, Gongye Liu, Jiajun Liang, Yangguang Li, Jiaheng Liu, Xintao Wang, Pengfei Wan, Di Zhang, and Wanli Ouyang. Flow-grpo: Training flow matching models via online rl. *arXiv preprint arXiv:2505.05470*, 2025.
- Xuantong Liu, Tianyang Hu, Wenjia Wang, Kenji Kawaguchi, and Yuan Yao. Referee can play: An alternative approach to conditional generation via model inversion. *arXiv preprint arXiv:2402.16305*, 2024.
- Cheng Lu, Yuhao Zhou, Fan Bao, Jianfei Chen, Chongxuan Li, and Jun Zhu. Dpm-solver: A fast ode solver for diffusion probabilistic model sampling in around 10 steps. *arXiv preprint arXiv:2206.00927*, 2022.
- Weijian Luo. A comprehensive survey on knowledge distillation of diffusion models. *arXiv preprint arXiv:2304.04262*, 2023.
- Weijian Luo. Diff-instruct++: Training one-step text-to-image generator model to align with human preferences. *arXiv preprint arXiv:2410.18881*, 2024.
- Weijian Luo, Tianyang Hu, Shifeng Zhang, Jiacheng Sun, Zhenguo Li, and Zhihua Zhang. Diff-instruct: A universal approach for transferring knowledge from pre-trained diffusion models. *Advances in Neural Information Processing Systems*, 36, 2023.
- Weijian Luo, Zemin Huang, Zhengyang Geng, J Zico Kolter, and Guo-jun Qi. One-step diffusion distillation through score implicit matching. *arXiv preprint arXiv:2410.16794*, 2024a.
- Weijian Luo, Colin Zhang, Debing Zhang, and Zhengyang Geng. Diff-instruct*: Towards human-preferred one-step text-to-image generative models. *arXiv preprint arXiv:2410.20898*, 2024b.
- Yihong Luo, Xiaolong Chen, Xinghua Qu, Tianyang Hu, and Jing Tang. You only sample once: Taming one-step text-to-image synthesis by self-cooperative diffusion gans, 2024c. URL <https://arxiv.org/abs/2403.12931>.
- Yihong Luo, Tianyang Hu, Weijian Luo, Kenji Kawaguchi, and Jing Tang. Reward-instruct: A reward-centric approach to fast photo-realistic image generation. *arXiv preprint arXiv:2503.13070*, 2025a.
- Yihong Luo, Tianyang Hu, Yifan Song, Jiacheng Sun, Zhenguo Li, and Jing Tang. Adding additional control to one-step diffusion with joint distribution matching. *arXiv preprint arXiv:2503.06652*, 2025b.
- Yihong Luo, Tianyang Hu, Jiacheng Sun, Yujun Cai, and Jing Tang. Learning few-step diffusion models by trajectory distribution matching. *arXiv preprint arXiv:2503.06674*, 2025c.
- Yihong Luo, Tianyang Hu, and Jing Tang. Reinforcing diffusion models by direct group preference optimization, 2025d. URL <https://arxiv.org/abs/2510.08425>.
- Yihong Luo, Shuchen Xue, Tianyang Hu, and Jing Tang. Noise consistency training: A native approach for one-step generator in learning additional controls. *arXiv preprint arXiv:2506.19741*, 2025e.
-

- Jiajun Ma, Tianyang Hu, Wenjia Wang, and Jiacheng Sun. Elucidating the design space of classifier-guided diffusion generation. *arXiv preprint arXiv:2310.11311*, 2023.
- Jiajun Ma, Shuchen Xue, Tianyang Hu, Wenjia Wang, Zhaoqiang Liu, Zhenguo Li, Zhi-Ming Ma, and Kenji Kawaguchi. The surprising effectiveness of skip-tuning in diffusion sampling. *arXiv preprint arXiv:2402.15170*, 2024.
- Yiyang Ma, Xingchao Liu, Xiaokang Chen, Wen Liu, Chengyue Wu, Zhiyu Wu, Zizheng Pan, Zhenda Xie, Haowei Zhang, Xingkai Yu, et al. Janusflow: Harmonizing autoregression and rectified flow for unified multimodal understanding and generation. In *Proceedings of the Computer Vision and Pattern Recognition Conference*, pages 7739–7751, 2025.
- Zichen Miao, Zhengyuan Yang, Kevin Lin, Ze Wang, Zicheng Liu, Lijuan Wang, and Qiang Qiu. Tuning timestep-distilled diffusion model using pairwise sample optimization, 2025. URL <https://arxiv.org/abs/2410.03190>.
- OpenAI. Dalle-2, 2023. URL <https://openai.com/dall-e-2>.
- Long Ouyang, Jeffrey Wu, Xu Jiang, Diogo Almeida, Carroll Wainwright, Pamela Mishkin, Chong Zhang, Sandhini Agarwal, Katarina Slama, Alex Ray, et al. Training language models to follow instructions with human feedback. *Advances in neural information processing systems*, 35:27730–27744, 2022.
- Dustin Podell, Zion English, Kyle Lacey, Andreas Blattmann, Tim Dockhorn, Jonas Müller, Joe Penna, and Robin Rombach. Sdxl: Improving latent diffusion models for high-resolution image synthesis. *arXiv preprint arXiv:2307.01952*, 2023.
- Mihir Prabhudesai, Anirudh Goyal, Deepak Pathak, and Katerina Fragkiadaki. Aligning text-to-image diffusion models with reward backpropagation. *arXiv preprint arXiv:2310.03739*, 2023.
- Yuxi Ren, Xin Xia, Yanzuo Lu, Jiacheng Zhang, Jie Wu, Pan Xie, Xing Wang, and Xuefeng Xiao. Hyper-sd: Trajectory segmented consistency model for efficient image synthesis. *arXiv preprint arXiv:2404.13686*, 2024.
- Robin Rombach, Andreas Blattmann, Dominik Lorenz, Patrick Esser, and Björn Ommer. High-resolution image synthesis with latent diffusion models. In *Proceedings of the IEEE/CVF Conference on Computer Vision and Pattern Recognition*, pages 10684–10695, 2022.
- Chitwan Saharia, William Chan, Saurabh Saxena, Lala Li, Jay Whang, Emily L Denton, Kamyar Ghasemipour, Raphael Gontijo Lopes, Burcu Karagol Ayan, Tim Salimans, et al. Photorealistic text-to-image diffusion models with deep language understanding. *Advances in neural information processing systems*, 35:36479–36494, 2022.
- Tim Salimans, Thomas Mensink, Jonathan Heek, and Emiel Hoogeboom. Multistep distillation of diffusion models via moment matching. *arXiv preprint arXiv:2406.04103*, 2024.
- Axel Sauer, Dominik Lorenz, Andreas Blattmann, and Robin Rombach. Adversarial diffusion distillation. *arXiv preprint arXiv:2311.17042*, 2023.
- Christoph Schuhmann, Romain Beaumont, Richard Vencu, Cade Gordon, Ross Wightman, Mehdi Cherti, Theo Coombes, Aarush Katta, Clayton Mullis, Mitchell Wortsman, et al. Laion-5b: An open large-scale dataset for training next generation image-text models. *Advances in Neural Information Processing Systems*, 35:25278–25294, 2022.
-

- Zhihong Shao, Peiyi Wang, Qihao Zhu, Runxin Xu, Junxiao Song, Xiao Bi, Haowei Zhang, Mingchuan Zhang, YK Li, Yang Wu, et al. Deepseekmath: Pushing the limits of mathematical reasoning in open language models. *arXiv preprint arXiv:2402.03300*, 2024.
- Chenyang Si, Ziqi Huang, Yuming Jiang, and Ziwei Liu. Freeu: Free lunch in diffusion u-net. In *Proceedings of the IEEE/CVF Conference on Computer Vision and Pattern Recognition*, pages 4733–4743, 2024.
- Jascha Sohl-Dickstein, Eric Weiss, Niru Maheswaranathan, and Surya Ganguli. Deep unsupervised learning using nonequilibrium thermodynamics. In *International Conference on Machine Learning*, pages 2256–2265. PMLR, 2015.
- Jiaming Song, Chenlin Meng, and Stefano Ermon. Denoising diffusion implicit models. *arXiv preprint arXiv:2010.02502*, 2020.
- Yang Song and Prafulla Dhariwal. Improved techniques for training consistency models. In *The Twelfth International Conference on Learning Representations*.
- Yang Song, Prafulla Dhariwal, Mark Chen, and Ilya Sutskever. Consistency models. *arXiv preprint arXiv:2303.01469*, 2023.
- Image Team, Huanqia Cai, Sihan Cao, Ruoyi Du, Peng Gao, Steven Hoi, Zhaohui Hou, Shijie Huang, Dengyang Jiang, Xin Jin, Liangchen Li, Zhen Li, Zhong-Yu Li, David Liu, Dongyang Liu, Junhan Shi, Qilong Wu, Feng Yu, Chi Zhang, Shifeng Zhang, and Shilin Zhou. Z-image: An efficient image generation foundation model with single-stream diffusion transformer, 2025. URL <https://arxiv.org/abs/2511.22699>.
- Bram Wallace, Meihua Dang, Rafael Rafailov, Linqi Zhou, Aaron Lou, Senthil Purushwalkam, Stefano Ermon, Caiming Xiong, Shafiq Joty, and Nikhil Naik. Diffusion model alignment using direct preference optimization. In *Proceedings of the IEEE/CVF Conference on Computer Vision and Pattern Recognition*, pages 8228–8238, 2024.
- Xinlong Wang, Xiaosong Zhang, Zhengxiong Luo, Quan Sun, Yufeng Cui, Jinsheng Wang, Fan Zhang, Yueze Wang, Zhen Li, Qiyang Yu, et al. Emu3: Next-token prediction is all you need. *arXiv preprint arXiv:2409.18869*, 2024.
- Yibin Wang, Yuhang Zang, Hao Li, Cheng Jin, and Jiaqi Wang. Unified reward model for multimodal understanding and generation. *arXiv preprint arXiv:2503.05236*, 2025a.
- Yifei Wang, Weimin Bai, Colin Zhang, Debing Zhang, Weijian Luo, and He Sun. Uni-instruct: One-step diffusion model through unified diffusion divergence instruction. *arXiv preprint arXiv:2505.20755*, 2025b.
- Zhengyi Wang, Cheng Lu, Yikai Wang, Fan Bao, Chongxuan Li, Hang Su, and Jun Zhu. Prolificdreamer: High-fidelity and diverse text-to-3d generation with variational score distillation. *arXiv preprint arXiv:2305.16213*, 2023.
- Xiaoshi Wu, Yiming Hao, Keqiang Sun, Yixiong Chen, Feng Zhu, Rui Zhao, and Hongsheng Li. Human preference score v2: A solid benchmark for evaluating human preferences of text-to-image synthesis. *arXiv preprint arXiv:2306.09341*, 2023.
- Enze Xie, Junsong Chen, Yuyang Zhao, Jincheng Yu, Ligeng Zhu, Chengyue Wu, Yujun Lin, Zhekai Zhang, Muyang Li, Junyu Chen, et al. Sana 1.5: Efficient scaling of training-time and inference-time compute in linear diffusion transformer. *arXiv preprint arXiv:2501.18427*, 2025.
-

- Jinheng Xie, Weijia Mao, Zechen Bai, David Junhao Zhang, Weihao Wang, Kevin Qinghong Lin, Yuchao Gu, Zhijie Chen, Zhenheng Yang, and Mike Zheng Shou. Show-o: One single transformer to unify multimodal understanding and generation. *arXiv preprint arXiv:2408.12528*, 2024a.
- Sirui Xie, Zhisheng Xiao, Diederik P Kingma, Tingbo Hou, Ying Nian Wu, Kevin Patrick Murphy, Tim Salimans, Ben Poole, and Ruiqi Gao. Em distillation for one-step diffusion models. *arXiv preprint arXiv:2405.16852*, 2024b.
- Jiazheng Xu, Xiao Liu, Yuchen Wu, Yuxuan Tong, Qinkai Li, Ming Ding, Jie Tang, and Yuxiao Dong. Imagereward: learning and evaluating human preferences for text-to-image generation. In *Proceedings of the 37th International Conference on Neural Information Processing Systems*, pages 15903–15935, 2023.
- Yanwu Xu, Yang Zhao, Zhisheng Xiao, and Tingbo Hou. Ufogen: You forward once large scale text-to-image generation via diffusion gans. In *Proceedings of the IEEE/CVF Conference on Computer Vision and Pattern Recognition*, pages 8196–8206, 2024.
- Shuchen Xue, Zhaoqiang Liu, Fei Chen, Shifeng Zhang, Tianyang Hu, Enze Xie, and Zhenguo Li. Accelerating diffusion sampling with optimized time steps. *arXiv preprint arXiv:2402.17376*, 2024.
- Shuchen Xue, Chongjian Ge, Shilong Zhang, Yichen Li, and Zhi-Ming Ma. Advantage weighted matching: Aligning rl with pretraining in diffusion models, 2025a. URL <https://arxiv.org/abs/2509.25050>.
- Zeyue Xue, Jie Wu, Yu Gao, Fangyuan Kong, Lingting Zhu, Mengzhao Chen, Zhiheng Liu, Wei Liu, Qiushan Guo, Weilin Huang, et al. Dancegrp: Unleashing grp on visual generation. *arXiv preprint arXiv:2505.07818*, 2025b.
- Kai Yang, Jian Tao, Jiafei Lyu, Chunjiang Ge, Jiabin Chen, Weihao Shen, Xiaolong Zhu, and Xiu Li. Using human feedback to fine-tune diffusion models without any reward model. In *Proceedings of the IEEE/CVF Conference on Computer Vision and Pattern Recognition*, pages 8941–8951, 2024.
- Zilyu Ye, Zhiyang Chen, Tiancheng Li, Zemin Huang, Weijian Luo, and Guo-Jun Qi. Schedule on the fly: Diffusion time prediction for faster and better image generation. *arXiv preprint arXiv:2412.01243*, 2024.
- Tianwei Yin, Michaël Gharbi, Richard Zhang, Eli Shechtman, Fredo Durand, William T Freeman, and Taesung Park. One-step diffusion with distribution matching distillation. *arXiv preprint arXiv:2311.18828*, 2023.
- Zhiyuan You, Xin Cai, Jinjin Gu, Tianfan Xue, and Chao Dong. Teaching large language models to regress accurate image quality scores using score distribution. In *Proceedings of the Computer Vision and Pattern Recognition Conference*, pages 14483–14494, 2025.
- Wenliang Zhao, Lujia Bai, Yongming Rao, Jie Zhou, and Jiwen Lu. Unipc: A unified predictor-corrector framework for fast sampling of diffusion models. *Advances in Neural Information Processing Systems*, 36:49842–49869, 2023.
- Kaiwen Zheng, Huayu Chen, Haotian Ye, Haoxiang Wang, Qinsheng Zhang, Kai Jiang, Hang Su, Stefano Ermon, Jun Zhu, and Ming-Yu Liu. Diffusionnft: Online diffusion reinforcement with forward process, 2025. URL <https://arxiv.org/abs/2509.16117>.
- Mingyuan Zhou, Huangjie Zheng, Zhendong Wang, Mingzhang Yin, and Hai Huang. Score identity distillation: Exponentially fast distillation of pretrained diffusion models for one-step generation. In *International Conference on Machine Learning*, 2024.
-

Daniel M Ziegler, Nisan Stiennon, Jeffrey Wu, Tom B Brown, Alec Radford, Dario Amodei, Paul Christiano, and Geoffrey Irving. Fine-tuning language models from human preferences. *arXiv preprint arXiv:1909.08593*, 2019.

A. Derivation

A.1. Derivation of Eq. (9)

For simplicity and without loss of generality, we omit the conditioning on \mathbf{c} throughout this derivation. By substituting the surrogate reward parameterization from Eq. (7) into the Bradley-Terry objective in Eq. (8), we obtain the initial training objective:

$$L(\phi) = -\mathbb{E}_k \mathbb{E}_{(\mathcal{G}_k^+, \mathcal{G}_k^-) \sim \mathcal{D}} \log \sigma \left(\sum_{\mathbf{x}_{t_k} \in \mathcal{G}_k^+} \mathbb{E}_{q(\mathbf{x}_{t_k+1:T} | \mathbf{x}_{t_k})} \beta w(\mathbf{x}_{t_k}) \left[\log \frac{p_\phi(\mathbf{x}_{t_k:T})}{p_{\text{ref}}(\mathbf{x}_{t_k:T})} + \log Z \right] \right. \\ \left. - \sum_{\mathbf{x}_{t_k} \in \mathcal{G}_k^-} \mathbb{E}_{q(\mathbf{x}_{t_k+1:T} | \mathbf{x}_{t_k})} \beta w(\mathbf{x}_{t_k}) \left[\log \frac{p_\phi(\mathbf{x}_{t_k:T})}{p_{\text{ref}}(\mathbf{x}_{t_k:T})} + \log Z \right] \right). \quad (12)$$

The partition function terms cancel because the weights sum to zero over the full group. Specifically, since the weights are defined as absolute normalized advantages and the partition into positive and negative groups is based on the sign of the advantage, we have $\sum_{\mathbf{x}_{t_k} \in \mathcal{G}_k^+} w(\mathbf{x}_{t_k}) - \sum_{\mathbf{x}_{t_k} \in \mathcal{G}_k^-} w(\mathbf{x}_{t_k}) = \sum_{\mathbf{x}_{t_k} \in \mathcal{G}_k} A(\mathbf{x}_{t_k}) = \sum_{\mathbf{x}_{t_k} \in \mathcal{G}_k} \frac{r(\mathbf{x}_{t_k}) - r_{\text{mean}}}{r_{\text{std}}} = 0$, where $r_{\text{mean}} = \frac{\sum_{\mathbf{x}_{t_k} \in \mathcal{G}_k} r(\mathbf{x}_{t_k})}{|\mathcal{G}|}$. This simplifies the objective to:

$$L(\phi) = -\mathbb{E}_{(\mathcal{G}^+, \mathcal{G}^-) \sim \mathcal{D}} \log \sigma \left(\beta \left[\sum_{\mathbf{x}_{t_k} \in \mathcal{G}^+} w(\mathbf{x}_{t_k}) \mathbb{E}_{q(\mathbf{x}_{t_k+1:T} | \mathbf{x}_{t_k})} \log \frac{p_\phi(\mathbf{x}_{t_k:T})}{p_{\text{ref}}(\mathbf{x}_{t_k:T})} \right. \right. \\ \left. \left. - \sum_{\mathbf{x}_{t_k} \in \mathcal{G}^-} w(\mathbf{x}_{t_k}) \mathbb{E}_{q(\mathbf{x}_{t_k+1:T} | \mathbf{x}_{t_k})} \log \frac{p_\phi(\mathbf{x}_{t_k:T})}{p_{\text{ref}}(\mathbf{x}_{t_k:T})} \right] \right). \quad (13)$$

Next, we decompose the trajectory-level log-ratio using the Markov property of the diffusion process. For any trajectory $\mathbf{x}_{t_k:T}$, the joint distribution factorizes as a product of transition probabilities:

$$\log \frac{p_\phi(\mathbf{x}_{t_k:T})}{p_{\text{ref}}(\mathbf{x}_{t_k:T})} = \sum_{t=t_k+1}^T \log \frac{p_\phi(\mathbf{x}_{t-1} | \mathbf{x}_t)}{p_{\text{ref}}(\mathbf{x}_{t-1} | \mathbf{x}_t)}. \quad (14)$$

Substituting this factorization and rewriting the sum over timesteps as an expectation, we obtain:

$$L(\phi) = -\mathbb{E}_{(\mathcal{G}^+, \mathcal{G}^-) \sim \mathcal{D}} \log \sigma \left(\beta (T - t_k) \mathbb{E}_{t \sim \mathcal{U}[t_k+1, T]} \mathbb{E}_{q(\mathbf{x}_t | \mathbf{x}_{t_k}), q(\mathbf{x}_{t-1} | \mathbf{x}_t, \mathbf{x}_{t_k})} \right. \\ \left. \times \left[\sum_{\mathbf{x}_{t_k} \in \mathcal{G}^+} w(\mathbf{x}_{t_k}) \log \frac{p_\phi(\mathbf{x}_{t-1} | \mathbf{x}_t)}{p_{\text{ref}}(\mathbf{x}_{t-1} | \mathbf{x}_t)} - \sum_{\mathbf{x}_{t_k} \in \mathcal{G}^-} w(\mathbf{x}_{t_k}) \log \frac{p_\phi(\mathbf{x}_{t-1} | \mathbf{x}_t)}{p_{\text{ref}}(\mathbf{x}_{t-1} | \mathbf{x}_t)} \right] \right). \quad (15)$$

To obtain a tractable upper bound, we apply Jensen's inequality. Since $-\log \sigma(\cdot)$ is a convex function, moving the expectation over t and $q(\mathbf{x}_t | \mathbf{x}_{t_k})$ inside the sigmoid yields:

$$L(\phi) \leq \mathbb{E}_{(\mathcal{G}^+, \mathcal{G}^-) \sim \mathcal{D}} \mathbb{E}_{t, q(\mathbf{x}_t | \mathbf{x}_{t_k})} \left[-\log \sigma \left(\beta (T - t_k) \mathbb{E}_{q(\mathbf{x}_{t-1} | \mathbf{x}_t, \mathbf{x}_{t_k})} \right. \right. \\ \left. \left. \times \left[\sum_{\mathbf{x}_{t_k} \in \mathcal{G}^+} w(\mathbf{x}_{t_k}) \log \frac{p_\phi(\mathbf{x}_{t-1} | \mathbf{x}_t)}{p_{\text{ref}}(\mathbf{x}_{t-1} | \mathbf{x}_t)} - \sum_{\mathbf{x}_{t_k} \in \mathcal{G}^-} w(\mathbf{x}_{t_k}) \log \frac{p_\phi(\mathbf{x}_{t-1} | \mathbf{x}_t)}{p_{\text{ref}}(\mathbf{x}_{t-1} | \mathbf{x}_t)} \right] \right) \right]. \quad (16)$$

Finally, we rewrite the log-ratios in terms of KL divergences. For any distribution q and models p_ϕ , p_{ref} , we have the following identity:

$$\mathbb{E}_{q(\mathbf{x}_{t-1}|\mathbf{x}_t, \mathbf{x}_{t_k})} \log \frac{p_\phi(\mathbf{x}_{t-1}|\mathbf{x}_t)}{p_{\text{ref}}(\mathbf{x}_{t-1}|\mathbf{x}_t)} = \text{KL}(q(\mathbf{x}_{t-1}|\mathbf{x}_t, \mathbf{x}_{t_k})\|p_{\text{ref}}(\mathbf{x}_{t-1}|\mathbf{x}_t)) - \text{KL}(q(\mathbf{x}_{t-1}|\mathbf{x}_t, \mathbf{x}_{t_k})\|p_\phi(\mathbf{x}_{t-1}|\mathbf{x}_t)). \quad (17)$$

Substituting this identity and rearranging terms, we arrive at the final upper bound:

$$\begin{aligned} L(\phi) \leq & \mathbb{E}_{(\mathcal{G}_k^+, \mathcal{G}_k^-) \sim \mathcal{D}_{k,k}} \mathbb{E}_{t,q(\mathbf{x}_t|\mathbf{x}_{t_k})} \log \sigma \left(-\beta(T - t_k) \left\{ \right. \\ & \sum_{\mathbf{x}_{t_k} \in \mathcal{G}_k^+} w(\mathbf{x}_{t_k}) \left[\text{KL}(q(\mathbf{x}_{t-1}|\mathbf{x}_t, \mathbf{x}_{t_k})\|p_\phi(\mathbf{x}_{t-1}|\mathbf{x}_t)) - \text{KL}(q(\mathbf{x}_{t-1}|\mathbf{x}_t, \mathbf{x}_{t_k})\|p_{\text{ref}}(\mathbf{x}_{t-1}|\mathbf{x}_t)) \right] \\ & \left. - \sum_{\mathbf{x}_{t_k} \in \mathcal{G}_k^-} w(\mathbf{x}_{t_k}) \left[\text{KL}(q(\mathbf{x}_{t-1}|\mathbf{x}_t, \mathbf{x}_{t_k})\|p_\phi(\mathbf{x}_{t-1}|\mathbf{x}_t)) - \text{KL}(q(\mathbf{x}_{t-1}|\mathbf{x}_t, \mathbf{x}_{t_k})\|p_{\text{ref}}(\mathbf{x}_{t-1}|\mathbf{x}_t)) \right] \right\} \right). \end{aligned} \quad (18)$$

This completes the derivation of Eq. (9).

A.2. Derivation of Eq. (11)

We compute the gradient of the objective in Eq. (10) by separately deriving the gradients of the reward maximization and KL regularization terms.

Step 1: Reformulating the Surrogate Reward. We first re-write the surrogate reward defined in Eq. (7) as follows:

$$\begin{aligned} \tilde{r}_\phi(\mathbf{x}_{t_k}, \mathbf{c}) &= \beta \mathbb{E}_{q(\mathbf{x}_{t_k+1:T}|\mathbf{x}_{t_k})} \log \frac{p_\phi(\mathbf{x}_{t_k:T}|\mathbf{c})}{p_{\text{ref}}(\mathbf{x}_{t_k:T}|\mathbf{c})} + \beta \log Z \\ &= \beta \mathbb{E}_{q(\mathbf{x}_{t_k+1:T}|\mathbf{x}_{t_k})} \sum_{t=t_k+1}^T \log \frac{p_\phi(\mathbf{x}_{t-1}|\mathbf{x}_t)}{p_{\text{ref}}(\mathbf{x}_{t-1}|\mathbf{x}_t)} + \beta \log Z. \end{aligned} \quad (19)$$

By converting the summation over timesteps into an expectation with respect to a uniform distribution over $t \geq t_k$, we obtain:

$$\begin{aligned} \tilde{r}_\phi(\mathbf{x}_{t_k}, \mathbf{c}) &= \beta(T - t_k) \mathbb{E}_{t \geq t_k} \mathbb{E}_{q(\mathbf{x}_{t_k+1:T}|\mathbf{x}_{t_k})} \log \frac{p_\phi(\mathbf{x}_{t-1}|\mathbf{x}_t)}{p_{\text{ref}}(\mathbf{x}_{t-1}|\mathbf{x}_t)} + \beta \log Z \\ &= \beta(T - t_k) \mathbb{E}_{t \geq t_k} \mathbb{E}_{q(\mathbf{x}_t|\mathbf{x}_{t_k})} \mathbb{E}_{q(\mathbf{x}_{t-1}|\mathbf{x}_t, \mathbf{x}_{t_k})} \log \frac{p_\phi(\mathbf{x}_{t-1}|\mathbf{x}_t)}{p_{\text{ref}}(\mathbf{x}_{t-1}|\mathbf{x}_t)} + \beta \log Z, \end{aligned} \quad (20)$$

where the last equality follows from marginalizing the joint distribution $q(\mathbf{x}_{t_k+1:T}|\mathbf{x}_{t_k})$ to the relevant variables \mathbf{x}_t and \mathbf{x}_{t-1} .

Step 2: Gradient of the Reward Term. Applying the chain rule through the reparameterized sampling process, the gradient of the reward term with respect to θ is given by:

$$\nabla_{\theta} \mathbb{E}_{k, p_\theta(\mathbf{x}_{t_k})} \tilde{r}_\phi(\mathbf{x}_{t_k}, \mathbf{c}) = \beta(T - t_k) \mathbb{E}_{k, t \geq t_k} \mathbb{E}_{p_\theta(\mathbf{x}_{t_k})} \mathbb{E}_{q(\mathbf{x}_t, \mathbf{x}_{t-1}|\mathbf{x}_{t_k})} \left[\nabla_{\mathbf{x}_t} \log \frac{p_\phi(\mathbf{x}_{t-1}|\mathbf{x}_t)}{p_{\text{ref}}(\mathbf{x}_{t-1}|\mathbf{x}_t)} \right] \frac{\partial \mathbf{x}_t}{\partial \mathbf{x}_{t_k}} \frac{\partial \mathbf{x}_{t_k}}{\partial \theta}. \quad (21)$$

Since the forward diffusion process $q(\mathbf{x}_t|\mathbf{x}_{t_k})$ is Gaussian with $\mathbf{x}_t = \alpha_{t|t_k} \mathbf{x}_{t_k} + \sigma_{t|t_k} \boldsymbol{\epsilon}$, where $\boldsymbol{\epsilon} \sim \mathcal{N}(\mathbf{0}, \mathbf{I})$, we have $\frac{\partial \mathbf{x}_t}{\partial \mathbf{x}_{t_k}} = \alpha_{t|t_k}$. Substituting this yields:

$$\nabla_{\theta} \mathbb{E}_{k, p_\theta(\mathbf{x}_{t_k})} \tilde{r}_\phi(\mathbf{x}_{t_k}, \mathbf{c}) = \beta(T - t_k) \mathbb{E}_{k, t \geq t_k} \mathbb{E}_{p_\theta(\mathbf{x}_{t_k})} \mathbb{E}_{q(\mathbf{x}_t, \mathbf{x}_{t-1}|\mathbf{x}_{t_k})} \left[\alpha_{t|t_k} \nabla_{\mathbf{x}_t} \log \frac{p_\phi(\mathbf{x}_{t-1}|\mathbf{x}_t)}{p_{\text{ref}}(\mathbf{x}_{t-1}|\mathbf{x}_t)} \right] \frac{\partial \mathbf{x}_{t_k}}{\partial \theta}. \quad (22)$$

Note that the gradient with respect to $\log Z$ vanishes since the partition function is independent of \mathbf{x}_t .

Step 3: Gradient of the KL Regularization Term. The gradient of the marginal-level KL divergence term follows from Eq. (2).

Step 4: Combining the Gradients. Combining the results from Steps 2 and 3, and incorporating the negative sign from the reward maximization term in Eq. (10), we arrive at the final gradient expression:

$$\nabla_{\theta} L(\theta) = -\mathbb{E}_{k,t \geq t_k} \mathbb{E}_{p_{\theta}(\mathbf{x}_{t_k})} \mathbb{E}_{q(\mathbf{x}_t, \mathbf{x}_{t-1} | \mathbf{x}_{t_k})} \left[\begin{aligned} & \beta \alpha_{t|t_k} (T - t_k) \nabla_{\mathbf{x}_t} \log \frac{p_{\phi}(\mathbf{x}_{t-1} | \mathbf{x}_t)}{p_{\text{ref}}(\mathbf{x}_{t-1} | \mathbf{x}_t)} \\ & + \beta_g \lambda_t (s_{\text{fake}}(\mathbf{x}_t) - s_{\psi}(\mathbf{x}_t)) \end{aligned} \right] \frac{\partial \mathbf{x}_{t_k}}{\partial \theta}, \quad (23)$$

which completes the derivation of Eq. (11).

B. Experiment details

Visual Text Rendering

Adopting the evaluation protocol from TextDiffuser (Chen et al., 2023) and the experimental framework of Flow-GRPO, we assess how accurately models can render textual content within generated images. Prompts follow a standardized template: “A sign that says ‘text’”, where ‘text’ denotes the target string to be visually rendered. Text fidelity (Gong et al., 2025) is computed as:

$$r = \max(1 - N_e / N_{\text{ref}}, 0)$$

Here, N_e represents the minimum edit distance between the rendered output and the target text, while N_{ref} indicates the character length of the quoted string in the prompt.

Setup Details

During training, we generate 24 samples per group. We employ Flow-DPM-Solver (Xie et al., 2025) with 4 sampling steps for both training rollouts and inference. We apply LoRA fine-tuning with rank 32, and set $\beta = 100$ as the default. Our default choice of β_g is set such that the ratio of the gradient of the reward term to the gradient of the KL regularization term is 2 : 1. All experiments are conducted at 512 resolution, with GPU hours reported in A100 equivalents.

Details of the out-of-domain evaluation metrics

We describe the specific out-of-domain metrics employed for quality assessment. The aesthetic score (Schuhmann et al., 2022) uses a CLIP-based linear regression model to quantify the visual appeal of generated images. To evaluate image quality degradation, we employ the DeQA score (You et al., 2025), which utilizes a multimodal large language model architecture to measure how various imperfections—such as distortions, textural degradation, and low-level visual artifacts—affect overall perceived image quality. ImageReward (Kirstain et al., 2023) assesses both visual quality and text-image correspondence, offering a holistic evaluation of generation quality from a human-centered standpoint. ImageReward (Xu et al., 2023) functions as a comprehensive human preference model for



Figure 10 | Qualitative comparisons of TDM-R1 against competing baselines. The same initial noise is used to generate all images.

text-to-image generation, evaluating multiple aspects including text-visual coherence and generation fidelity. Lastly, UnifiedReward (Wang et al., 2025a) represents a state-of-the-art advancement in this domain. This unified reward framework is capable of evaluating both multimodal understanding and generation tasks, and has achieved superior performance on human preference assessment benchmarks compared to prior methods.

C. Additional Qualitative Comparison

We present additional visual comparison in Fig. 10.